Hindawi Publishing Corporation
Mathematical Problems in Engineering
Volume 2012, Article ID 815747, 23 pages
doi:10.1155/2012/815747

Research Article

Peristaltic Slip Flow of a Viscoelastic Fluid with Heat and Mass Transfer in a Tube

Ayman Mahmoud Sobh

Institute of Fluid Mechanics, TU Braunschweig, Braunschweig, Germany

Correspondence should be addressed to Ayman Mahmoud Sobh, aymansobh@yahoo.com

Received 26 July 2012; Revised 23 October 2012; Accepted 8 November 2012

Academic Editor: Anuar Ishak

The paper discusses the combined effect of slip velocity and heat and mass transfer on peristaltic flow of a viscoelastic fluid in a uniform tube. This study has numerous applications. It serves as a model for the chyme movement in the small intestine, by considering the chyme as a viscoelastic fluid. The problem is formulated and analysed using perturbation expansion in terms of the wave number as a parameter. Analytic solutions for the axial velocity component, pressure gradient, temperature distribution, and fluid concentration are derived. Also, the effects of the emerging parameters on pressure gradient, temperature distribution, concentration profiles, and trapping phenomenon are illustrated graphically and discussed in detail.

1. Introduction

Peristalsis is an important mechanism for mixing and transporting fluid which is generated by a progressive wave of contraction or expansion moving on the wall of the tube. It occurs widely in many biological and biomedical systems. In physiology, it plays an indispensable role in various situations. For examples, the transport of urine from kidney to the bladder, the movement of chyme in the gastrointestinal tract, transport of spermatozoa in the ducts efferentes of the male reproductive tracts, movement of ovum in the female fallopian tube, transport of lymph in the lymphatic vessels, vasomotion of small blood vessels such as arterioles, venules, and capillaries, and so on.

The peristaltic flow of non-Newtonian fluids has gained considerable interest during the recent years because of its applications in industry and biology. In biology, it is well known that most physiological fluids behave like non-Newtonian fluids. Hence, the study

of peristaltic transport of non-Newtonian fluids may help to get a better understanding for some biological systems. Now, several theoretical and numerical investigations have been carried out to understand the peristaltic mechanism in different situations. Some of the recent studies on peristaltic flow of non-Newtonian Fluids can be seen through references [1–10].

Recently, investigations of heat and mass transfer in peristalsis have been considered by some researchers due to its applications in the biomedical sciences. Srinivas and Kothandapani [11] investigated the influence of heat and mass transfer on MHD peristaltic flow through a porous space with compliant walls. Eldabe et al. [12] studied the mixed convective heat and mass transfer in a non-Newtonian fluid at a peristaltic surface with temperature-dependent viscosity. The influence of radially varying MHD on the peristaltic flow in an annulus with heat and mass transfer has been studied by Nadeem and Akbar [13]. Moreover, Akbar et al. [14] investigated the effect of heat and mass transfer on the peristaltic flow of hyperbolic tangent fluid in an annulus. Moreover, Hayat et al. [15] investigated the peristaltic flow of pseudoplastic fluid under the effects of an induced magnetic field and heat and mass transfer in a channel. Furthermore, Hayat et al. [16] studied the heat and mass transfer effects on the peristaltic flow of Johnson-Segalman fluid in a curved channel with compliant walls.

Problems that involve slip boundary conditions may be useful models for flows through pipes in which chemical reactions occur at the walls, flows with laminar film condensation, and certain two phase flows. Motivated by this, several studies were made to investigate the effect of slip velocity on peristaltic transport. Some of these studies have been done by Sobh [17], Hayat and Mehmood [18], Noreen et al. [19], Hayat et al. [20], and Saleem et al. [21].

It is noticed from the available literature that no analysis has been made yet for the peristaltic flow of a viscoelastic fluid with heat and mass transfer in a tube in the presence of slip conditions on the tube wall. For this purpose, the peristaltic slip flow of an Oldroyd fluid, as a viscoelastic fluid, in a uniform tube is considered here in the presence of heat and mass transfer. This analysis can model movement of the chyme in the small intestine by considering chyme as an Oldroyd fluid. The flow analysis is developed in a wave frame of reference moving with the same velocity of the wave travelling down the tube wall. The perturbation technique is used to obtain an analytic solution for the governing equations in terms of the wave, Reynolds, and Weissenberg numbers. The derived solutions for pressure gradient, temperature field, and concentration profiles are plotted and analyzed in detail. The trapping phenomenon is also discussed.

2. Mathematical Modeling

The continuity and momentum equations for an incompressible fluid, in the absence of body forces, are given by

$$\begin{aligned} \operatorname{div} \mathbf{V} &= 0, \\ \rho \frac{d\mathbf{V}}{dt} &= -\nabla p + \operatorname{div} \boldsymbol{\tau}, \end{aligned} \tag{2.1}$$

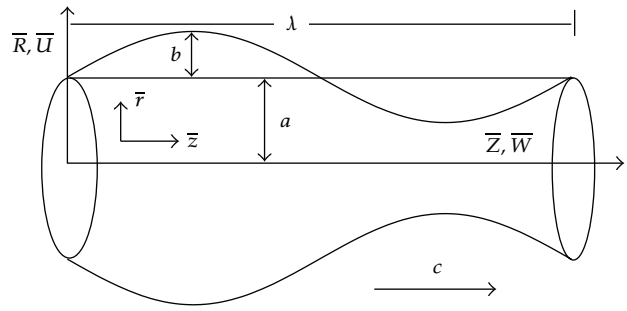

Figure 1: Geometry of the problem.

where ρ is the density of the fluid, $\mathbf{V}$ is the velocity vector, p is the pressure, $\boldsymbol{\tau}$ is the extra stress tensor, and d/dt is the material time derivative. The constitutive equation for Oldroyd fluid is given by [22]

$$\tau_{ij} + \Gamma\left[\frac{\partial \tau_{ij}}{\partial t} + \sqrt{(g^{kk}g_{ii}g_{jj})}v_k \frac{\partial}{\partial x^k}\left(\sqrt{g^{ii}g^{jj}}\tau_{ij}\right) - \sqrt{g^{kk}g_{jj}}\tau_{kj}\frac{\partial}{\partial x_k}\left(\sqrt{g^{ii}}v_i\right) - \sqrt{g^{kk}g_{ii}}\tau_{ik}\frac{\partial}{\partial x_k}\left(\sqrt{g^{jj}}v_j\right)\right] = -\mu\dot{\gamma}_{ij}, \tag{2.2}$$

in which $\tau_{ij}, i, j, k = 1, 2, 3$ are the components of the extra stress tensor, g_{ii} and g^{jj} are respectively the diagonal components of covariant and contravariant metric tensor, v_i are the velocity components, μ is the fluid viscosity, Γ is relaxation time, and $\dot{\gamma}_{ij}$ are the components of strain-rate tensor.

3. Formulation of the Problem

Consider the peristaltic flow of an incompressible Oldroyd fluid in an axisymmetric tube of a sinusoidal wave travelling down its wall. The wall of the tube is maintained at temperature $\overline{T}_0$ and concentration $\overline{C}_0$. In the fixed cylindrical coordinate system $(\overline{R}, \overline{Z})$, the geometry of the problem, as can be seen in Figure 1, is

$$\overline{h}\left(\overline{Z}, \overline{t}\right) = a + b\ \sin\left[\frac{2\pi}{\lambda}\left(\overline{Z} - c\overline{t}\right)\right], \tag{3.1}$$

where $\overline{Z}$ is the axis lies along the centreline of the tube, $\overline{R}$ is the distance measured radially, a is the radius of the tube, b is the wave amplitude, λ is the wavelength, and c is the propagation velocity.

Let us introduce a wave frame $(\overline{r},\overline{z})$ moving with velocity c away from the fixed frame $(\overline{R},\overline{Z})$ by the transformation

$$\begin{aligned} \overline{r} &= \overline{R}, \qquad \overline{z} = \overline{Z} - c\overline{t}, \\ \overline{u} &= \overline{U}, \qquad \overline{w} = \overline{W} - c, \end{aligned} \tag{3.2}$$

where $(\overline{U},\overline{W})$, $(\overline{u},\overline{w})$ are the velocity components in the fixed and wave frames, respectively. For the case of axisymmetric tube, the constitutive equations (2.2), in the wave frame, become

$$\begin{aligned} \overline{\tau}_{11} + \Gamma\left(\overline{u}\frac{\partial\overline{\tau}_{11}}{\partial\overline{r}} + \overline{w}\frac{\partial\overline{\tau}_{11}}{\partial\overline{z}} - 2\overline{\tau}_{11}\frac{\partial\overline{u}}{\partial\overline{r}} - 2\overline{\tau}_{13}\frac{\partial\overline{u}}{\partial\overline{z}}\right) &= -\mu\overline{\dot{\gamma}}_{11}, \\ \overline{\tau}_{13} + \Gamma\left(\overline{u}\frac{\partial\overline{\tau}_{13}}{\partial\overline{r}} + \overline{w}\frac{\partial\overline{\tau}_{13}}{\partial\overline{z}} - \overline{\tau}_{33}\frac{\partial\overline{u}}{\partial\overline{z}} - \overline{\tau}_{11}\frac{\partial\overline{w}}{\partial\overline{r}} + \frac{\overline{u}}{\overline{r}}\overline{\tau}_{13}\right) &= -\mu\overline{\dot{\gamma}}_{13}, \\ \overline{\tau}_{22} + \Gamma\left(\overline{u}\frac{\partial\overline{\tau}_{22}}{\partial\overline{r}} + \overline{w}\frac{\partial\overline{\tau}_{22}}{\partial\overline{z}} - 2\frac{\overline{u}}{\overline{r}}\overline{\tau}_{22}\right) &= -\mu\overline{\dot{\gamma}}_{22}, \\ \overline{\tau}_{33} + \Gamma\left(\overline{u}\frac{\partial\overline{\tau}_{33}}{\partial\overline{r}} + \overline{w}\frac{\partial\overline{\tau}_{33}}{\partial\overline{z}} - 2\overline{\tau}_{33}\frac{\partial\overline{w}}{\partial\overline{z}} - 2\overline{\tau}_{13}\frac{\partial\overline{w}}{\partial\overline{r}}\right) &= -\mu\overline{\dot{\gamma}}_{33}, \end{aligned} \tag{3.3}$$

where the components of the strain-rate tensor are given by

$$\overline{\dot{\gamma}}_{11} = 2\frac{\partial\overline{u}}{\partial\overline{r}}, \qquad \overline{\dot{\gamma}}_{22} = 2\frac{\overline{u}}{\overline{r}}, \qquad \overline{\dot{\gamma}}_{33} = 2\frac{\partial\overline{w}}{\partial\overline{z}}, \qquad \overline{\dot{\gamma}}_{13} = \left(\frac{\partial\overline{u}}{\partial\overline{z}} + \frac{\partial\overline{w}}{\partial\overline{r}}\right). \tag{3.4}$$

Using the following non-dimensional variables and parameters:

$$\begin{aligned} r &= \frac{\overline{r}}{a}, \qquad z = \frac{\overline{z}}{\lambda}, \qquad w = \frac{\overline{w}}{c}, \qquad u = \frac{\lambda\overline{u}}{ac}, \\ \dot{\gamma}_{ij} &= \frac{a}{c}\overline{\dot{\gamma}}_{ij}, \qquad p = \frac{a^2\overline{p}}{c\lambda\mu}, \qquad t = \frac{c\overline{t}}{\lambda}, \qquad \delta = \frac{a}{\lambda}, \\ \mathrm{Re} &= \frac{\rho ca}{\mu}, \qquad \tau_{ij} = \frac{a\overline{\tau}_{ij}}{c\mu}, \qquad \mathrm{Wi} = \frac{c\Gamma}{a}, \qquad T = \frac{\overline{T}}{\overline{T}_0}, \\ C &= \frac{\overline{C}}{\overline{C}_0}, \qquad Pr = \frac{\mu c_p}{k}, \qquad E = \frac{c^2}{\overline{T}_0 c_p}, \\ \mathrm{Sr} &= \frac{\rho D_m K_T \overline{T}_0}{\mu T_m \overline{C}_0}, \qquad \mathrm{Sc} = \frac{\mu}{\rho D_m}, \qquad h = \frac{\overline{h}}{a} = 1 + \frac{b}{a}\sin 2\pi z = 1 + \varphi\sin 2\pi z, \end{aligned} \tag{3.5}$$

we obtain the non-dimensional continuity equation, momentum equations, constitutive equations, energy equation, and concentration equation as follows:

$$\begin{aligned}
\frac{1}{r}\frac{\partial}{\partial r}(ru) + \frac{\partial w}{\partial z} &= 0,\\
\operatorname{Re}\delta^3\left(u\frac{\partial u}{\partial r} + w\frac{\partial u}{\partial z}\right) &= -\frac{\partial p}{\partial z} - \delta\left(\frac{1}{r}\frac{\partial}{\partial r}(r\tau_{11}) + \delta\frac{\partial \tau_{13}}{\partial z} - \frac{\tau_{22}}{r}\right),\\
\operatorname{Re}\delta\left(u\frac{\partial w}{\partial r} + w\frac{\partial w}{\partial z}\right) &= -\frac{\partial p}{\partial z} - \left(\frac{1}{r}\frac{\partial}{\partial r}(r\tau_{13}) + \delta\frac{\partial \tau_{33}}{\partial z}\right),\\
\tau_{11} + \delta\mathrm{Wi}\left[u\frac{\partial \tau_{11}}{\partial r} + w\frac{\partial \tau_{11}}{\partial z} - 2\tau_{11}\frac{\partial u}{\partial r} - 2\delta\tau_{13}\frac{\partial u}{\partial z}\right] &= -2\delta\left(\frac{\partial u}{\partial r}\right),\\
\tau_{13} + \mathrm{Wi}\left[\delta\left(u\frac{\partial \tau_{13}}{\partial r} + w\frac{\partial \tau_{13}}{\partial z} - \delta\tau_{33}\frac{\partial u}{\partial z} + \frac{u}{r}\tau_{13}\right) - \tau_{11}\frac{\partial w}{\partial r}\right] &= -\left(\delta^2\frac{\partial u}{\partial z} + \frac{\partial w}{\partial r}\right),\\
\tau_{22} + \delta\mathrm{Wi}\left[u\frac{\partial \tau_{22}}{\partial r} + w\frac{\partial \tau_{22}}{\partial z} - \frac{2u}{r}\tau_{22}\right] &= -2\delta\frac{u}{r},\\
\tau_{33} + Wi\left[\delta\left(u\frac{\partial \tau_{33}}{\partial r} + w\frac{\partial \tau_{33}}{\partial z} - 2\tau_{33}\frac{\partial w}{\partial z}\right) - 2\tau_{13}\frac{\partial w}{\partial r}\right] &= -2\delta\left(\frac{\partial w}{\partial z}\right),\\
\delta\mathrm{Pr}\left(u\frac{\partial T}{\partial r} + w\frac{\partial T}{\partial z}\right) &= \left(\frac{1}{r}\frac{\partial}{\partial r}\left(r\frac{\partial T}{\partial r}\right) + \delta^2\frac{\partial^2 T}{\partial z^2}\right)\\
&\quad - \mathrm{Br}\left(\delta\tau_{11}\frac{\partial u}{\partial r} + \tau_{13}\frac{\partial w}{\partial r} + \delta^2\tau_{31}\frac{\partial u}{\partial z} + \delta\tau_{33}\frac{\partial w}{\partial z}\right),\\
\delta\operatorname{Re}\left(u\frac{\partial C}{\partial r} + w\frac{\partial C}{\partial z}\right) &= \frac{1}{\mathrm{Sc}}\left(\frac{1}{r}\frac{\partial}{\partial r}\left(r\frac{\partial C}{\partial r}\right) + \delta^2\frac{\partial^2 C}{\partial z^2}\right)\\
&\quad + \mathrm{Sr}\left(\frac{1}{r}\frac{\partial}{\partial r}\left(r\frac{\partial T}{\partial r}\right) + \delta^2\frac{\partial^2 T}{\partial z^2}\right),
\end{aligned} \tag{3.6}$$

where C is the concentration of the fluid, T is the temperature, T_m is the temperature of the medium, D_m is the coefficient of mass diffusivity, K_T is the thermal diffusion ratio, μ is the viscosity, c_p is the specific heat at constant volume, k is the thermal conductivity, δ is the dimensionless wave number assumed to be small, Re is the Reynolds number, Wi is the Weissenberg number, Pr is the Prandtl number, E is the Eckert number, Sr is the Soret number, Sc is the Schmidt number, and $\mathrm{Br} = E\ \mathrm{Pr}$ is the Brinkman number.

The dimensionless boundary conditions are

$$\begin{aligned}
&u = 0, \qquad \frac{\partial w}{\partial r} = 0, \qquad \frac{\partial T}{\partial r} = 0, \qquad \frac{\partial C}{\partial r} = 0, \quad \text{at } r = 0,\\
&w = -1 + K_n\tau_{13}, \qquad u = \frac{dh}{dz}, \qquad T = 1, \qquad C = 1, \quad \text{at } r = h,
\end{aligned} \tag{3.7}$$

where $K_n = \overline{K}_n/a$, is the dimensionless slip parameter.

4. Perturbation Solution

We begin the construction of the solution by expanding the following quantities as power series in the small parameter δ as follows:

$$\begin{aligned}
w &= w_0 + \delta w_1 + \delta^2 w_2 + O\left(\delta^3\right),\\
u &= u_0 + \delta u_1 + \delta^2 u_2 + O\left(\delta^3\right),\\
p &= p_0 + \delta p_1 + \delta^2 p_2 + O\left(\delta^3\right),\\
f &= f_0 + \delta f_1 + \delta^2 f_2 + O\left(\delta^3\right),\\
\tau_{ij} &= \tau_{ij}^{(0)} + \delta\tau_{ij}^{(1)} + \delta^2\tau_{ij}^{(2)} + O\left(\delta^3\right), \quad i,j = 1,2,3,\\
T &= T_0 + \delta T_1 + \delta^2 T_2 + O\left(\delta^3\right),\\
C &= C_0 + \delta C_1 + \delta^2 C_2 + O\left(\delta^3\right),
\end{aligned} \tag{4.1}$$

where $f = 2\int_0^h rwdr$ is the dimensionless mean flow rate in the wave frame which is related with the mean flow rate in the fixed frame θ by the relation [4]

$$\theta = f + \left(1 + \frac{\varphi^2}{2}\right). \tag{4.2}$$

Substituting the expansions (4.1) into (3.6) and (3.7) and collecting terms of like powers of δ we obtain the following systems of coupled differential equations.

4.1. Zero Order System

Consider

$$\begin{aligned}
\frac{1}{r}\frac{\partial}{\partial r}(ru_0) + \frac{\partial w_0}{\partial z} &= 0,\\
\frac{\partial p_0}{\partial r} &= 0,\\
\frac{\partial p_0}{\partial z} &= \frac{1}{r}\frac{\partial}{\partial r}\left(r\frac{\partial w_0}{\partial r}\right),\\
\frac{1}{r}\frac{\partial}{\partial r}\left(r\frac{\partial T_0}{\partial r}\right) &= -\mathrm{Br}\left(\frac{\partial w_0}{\partial r}\right)^2,\\
0 &= \frac{1}{\mathrm{Sc}}\left(\frac{1}{r}\frac{\partial}{\partial r}\left(r\frac{\partial C_0}{\partial r}\right)\right) + \mathrm{Sr}\left(\frac{1}{r}\frac{\partial}{\partial r}\left(r\frac{\partial T_0}{\partial r}\right)\right),
\end{aligned} \tag{4.3}$$

with the boundary conditions

$$\begin{aligned} &\frac{\partial w_0}{\partial r} = 0, \qquad \frac{\partial T_0}{\partial r} = 0, \qquad \frac{\partial C_0}{\partial r} = 0, \quad \text{at } r = 0, \\ &w_0 = -1 - K_n\left(\frac{\partial w_0}{\partial r}\right), \qquad T_0 = 1, \qquad C_0 = 1, \quad \text{at } r = h(z). \end{aligned} \tag{4.4}$$

The solution of (4.3), subject to the boundary conditions (4.4), is

$$\begin{aligned} w_0(r,z) &= a_1 r^2 + a_2, \\ u_0(r,z) &= a_3 r^3 + a_4 r, \\ \frac{dp_0}{dz} &= -\frac{8\left(f_0 + h^2\right)}{\left(h^4 + 4h^3 K_n\right)}. \\ T_0(r,z) &= -\mathrm{Br}\left[\frac{1}{64}\left(\frac{dp_0}{dz}\right)^2\left(r^4 - h^4\right)\right] + 1, \\ C_0(r,z) &= \mathrm{Sr}\ \mathrm{Sc}\ \mathrm{Br}\left[\frac{1}{64}\left(\frac{dp_0}{dz}\right)^2\left(r^4 - h^4\right)\right] + 1, \end{aligned} \tag{4.5}$$

where a_1, a_2, a_3, and a_4 are stated in the appendix.

4.2. First Order System

Consider

$$\frac{1}{r}\frac{\partial}{\partial r}(r u_1) + \frac{\partial w_1}{\partial z} = 0, \tag{4.6}$$

$$\frac{\partial p_1}{\partial r} = 0, \tag{4.7}$$

$$\mathrm{Re}\left(u_0\frac{\partial w_0}{\partial r} + w_0\frac{\partial w_0}{\partial z}\right) = -\frac{\partial p_1}{\partial z} - \frac{1}{r}\frac{\partial}{\partial r}\left(r\tau_{13}^{(1)}\right) + 2\mathrm{Wi}\frac{\partial}{\partial z}\left[\left(\frac{\partial w_0}{\partial r}\right)^2\right], \tag{4.8}$$

$$\tau_{13}^{(1)} = -\left(\frac{\partial w_1}{\partial r}\right) + \mathrm{Wi}\left[u_0\frac{\partial^2 w_0}{\partial r^2} + w_0\frac{\partial^2 w_0}{\partial r \partial z} + \frac{u_0}{r}\frac{\partial w_0}{\partial r} - 2\left(\frac{\partial u_0}{\partial r}\right)\left(\frac{\partial w_0}{\partial r}\right)\right], \tag{4.9}$$

$$\begin{aligned} \frac{1}{r}\frac{\partial}{\partial r}\left(r\ \frac{\partial T_1}{\partial r}\right) = {} & \mathrm{Re}\ \mathrm{Pr}\left(u_0\frac{\partial T_0}{\partial r} + w_0\frac{\partial T_0}{\partial z}\right) \\ & + \mathrm{Br}\left[\tau_{13}^{(1)}\frac{\partial w_0}{\partial r} - \left(\frac{\partial w_0}{\partial r}\right)\left(\frac{\partial w_1}{\partial r}\right) - 2\mathrm{Wi}\left(\frac{\partial w_0}{\partial r}\right)^2\left(\frac{\partial w_0}{\partial z}\right)\right], \end{aligned} \tag{4.10}$$

$$\mathrm{Re}\ \left(u_0\frac{\partial C_0}{\partial r} + w_0\frac{\partial C_0}{\partial z}\right) = \frac{1}{\mathrm{Sc}}\left(\frac{1}{r}\frac{\partial}{\partial r}\left(r\frac{\partial C_1}{\partial r}\right)\right) + \mathrm{Sr}\left(\frac{1}{r}\frac{\partial}{\partial r}\left(r\frac{\partial T_1}{\partial r}\right)\right). \tag{4.11}$$

The boundary conditions are

$$\frac{\partial w_1}{\partial r} = 0, \qquad \frac{\partial T_1}{\partial r} = 0, \qquad \frac{\partial C_1}{\partial r} = 0, \quad \text{at } r = 0, \tag{4.12}$$

$$w_1 = K_n \tau_{13}^{(1)}, \qquad T_1 = 0, \qquad C_1 = 0 \quad \text{at } r = h(z). \tag{4.13}$$

Substituting the zero order solution into (4.9), we obtain $\tau_{13}^{(1)}$ in the form

$$\tau_{13}^{(1)} = -\left(\frac{\partial w_1}{\partial r}\right) + Wi\left[\left(2a_1 a_1' - 8a_1 a_3\right) r^3 + \left(2a_2 a_1'\right) r\right]. \tag{4.14}$$

Substituting (4.14) together with the zero order solution into (4.8) and integrating subject to the boundary condition (4.12), taking into account that $\partial p_1/\partial r = 0$, we obtain a differential equation for $w_1(r,z)$ in the form

$$\begin{aligned}\frac{\partial w_1}{\partial r} = {} & \frac{1}{2}\left(\frac{dp_1}{dz}\right) r + \mathrm{Wi}\left[-2\left(4a_1 a_3 + a_1 a_1'\right) r^3 + 2a_2 a_1' r\right] \\ & + \mathrm{Re}\left[\frac{\left(2a_1 a_3 + a_1 a_1'\right)}{6} r^5 + \frac{\left(2a_1 a_4 + a_1 a_2' + a_2 a_1'\right)}{4} r^3 + \frac{a_2 a_2'}{2} r\right].\end{aligned} \tag{4.15}$$

The solution of (4.15), subject to the boundary condition (4.13) is given by

$$\begin{aligned}w_1(r,z) = {} & \frac{1}{4}\left(\frac{dp_1}{dz}\right)\left(r^2 - h^2 - 2K_n h\right) + \mathrm{Re}\left(a_5 r^6 + a_6 r^4 + a_7 r^2 + a_8\right) \\ & + \mathrm{Wi}\left(a_9 r^4 + a_{10} r^2 + a_{11}\right),\end{aligned} \tag{4.16}$$

where $a_5, \ldots a_{11}$ are stated in the appendix.

The dimensionless mean flow rate in the wave frame f_1 is given by

$$\begin{aligned}f_1 = 2\int_0^h r w_1 dr = {} & -\frac{1}{8}\left(\frac{dp_1}{dz}\right) h^4 + \mathrm{Re}\left[\frac{a_5}{4} h^8 + \frac{a_6}{3} h^6 + \frac{a_7}{2} h^4 + a_8 h^2\right] \\ & + \mathrm{Wi}\left[\frac{a_9}{3} h^6 + \frac{a_{10}}{2} h^4 + a_{11} h^2\right].\end{aligned} \tag{4.17}$$

On solving (4.17) for dp_1/dz, one finds

$$\begin{aligned}\frac{dp_1}{dz} = {} & -\frac{8 f_1}{\left(h^4 + 4K_n h^3\right)} - \frac{\mathrm{Re}}{\left(h^4 + 4K_n h^3\right)}\left(2a_5 h^8 + \frac{8}{3} a_6 h^6 + 4a_7 h^4 + 8a_8 h^2\right) \\ & - \frac{\mathrm{Wi}}{\left(h^4 + 4K_n h^3\right)}\left(\frac{8}{3} a_9 h^6 + 4a_{10} h^4 + 8a_{11} h^2\right).\end{aligned} \tag{4.18}$$

Using zero order solution together with the first order solution of $w_1(r,z)$, (4.16), into (4.10), (4.11) and applying the boundary conditions, we get

$$\begin{aligned} T_1(r,z) = & -\frac{\mathrm{Br}}{32}\left(\frac{dp_0}{dz}\right)\left(\frac{dp_1}{dz}\right)\left(r^4-h^4\right) \\ & -\mathrm{Br}\ \mathrm{Re}\left[a_{12}\left(r^8-h^8\right)+a_{13}\left(r^6-h^6\right)+a_{14}\left(r^4-h^4\right)+a_{15}\left(r^2-h^2\right)\right] \\ & -\mathrm{Br}\ \mathrm{Wi}\left[a_{16}\left(r^6-h^6\right)+a_{17}\left(r^5-h^5\right)+a_{18}\left(r^4-h^4\right)+a_{19}\left(r^3-h^3\right)\right], \end{aligned} \tag{4.19}$$

$$\begin{aligned} C_1(r,z) = & \frac{\mathrm{Br}\ \mathrm{Sr}\ \mathrm{Sc}}{32}\left(\frac{dp_0}{dz}\right)\left(\frac{dp_1}{dz}\right)\left(r^4-h^4\right) \\ & +\mathrm{Br}\ \mathrm{Sr}\ \mathrm{ScRe}\left[a_{20}\left(r^8-h^8\right)+a_{21}\left(r^6-h^6\right)+a_{22}\left(r^4-h^4\right)+a_{23}\left(r^2-h^2\right)\right] \\ & +\mathrm{Br}\ \mathrm{Sr}\ \mathrm{Sc}\ \mathrm{Wi}\left[a_{16}\left(r^6-h^6\right)+a_{17}\left(r^5-h^5\right)+a_{18}\left(r^4-h^4\right)+a_{19}\left(r^3-h^3\right)\right], \end{aligned} \tag{4.20}$$

where $a_{12},\ldots a_{19}$ are defined in the appendix.

The results of our analysis can be expressed to first order by defining

$$f = f + \delta f_1, \tag{4.21}$$

then substituting into zero and first order solutions and neglecting all terms of higher than $O(\delta)$, we find

$$\begin{aligned} w(r,z) = & \frac{1}{4}\left(\frac{dp}{dz}\right)\left(r^2-h^2-2K_nh\right)-1+\delta\,\mathrm{Re}\left(b_5r^6+b_6r^4+b_7r^2+b_8\right) \\ & +\delta\mathrm{Wi}\left(b_9r^4+b_{10}r^2+b_{11}\right), \\ \frac{dp}{dz} = & -\frac{(8f+h^2)}{\left(h^4+4K_nh^3\right)}-\frac{\delta\,\mathrm{Re}}{\left(h^4+4K_nh^3\right)}\left(2b_5h^8+\frac{8}{3}b_6h^6+4b_7h^4+8b_8h^2\right) \\ & -\frac{\delta\mathrm{Wi}}{\left(h^4+4K_nh^3\right)}\left(\frac{8}{3}b_9h^6+4b_{10}h^4+8b_{11}h^2\right), \\ T(r,z) = & -\frac{\mathrm{Br}}{64}\left(\frac{dp}{dz}\right)^2\left(r^4-h^4\right)+1 \\ & -\delta\mathrm{Br}\left[\mathrm{Re}\left\{b_{12}\left(r^8-h^8\right)+b_{13}\left(r^6-h^6\right)+b_{14}\left(r^4-h^4\right)+b_{15}\left(r^2-h^2\right)\right\}\right. \\ & \left.+\mathrm{Wi}\left\{b_{16}\left(r^6-h^6\right)+b_{17}\left(r^5-h^5\right)+b_{18}\left(r^4-h^4\right)+b_{19}\left(r^3-h^3\right)\right\}\right], \end{aligned}$$

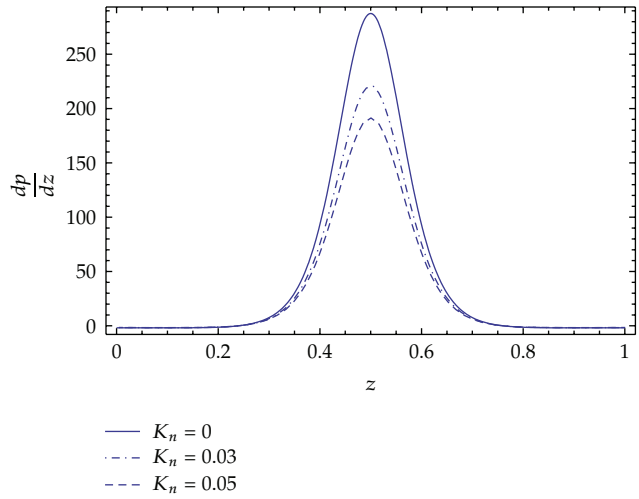

Figure 2: Pressure gradient versus z for $\phi = 0.6$, Wi = 0, Re = 0, $\delta = 0$, $\theta = 0.1$.

$$C(r,z) = \frac{\text{Br Sr Sc}}{64}\left(\frac{dp}{dz}\right)^2\left(r^4 - h^4\right) + 1 + \delta\text{Br Sr Sc}\Big[\text{Re}\Big\{b_{20}\left(r^8 - h^8\right) + b_{21}\left(r^6 - h^6\right) + b_{22}\left(r^4 - h^4\right) + b_{23}\left(r^2 - h^2\right)\Big\} + \text{Wi}\Big\{b_{16}\left(r^6 - h^6\right) + b_{17}\left(r^5 - h^5\right) + b_{18}\left(r^4 - h^4\right) + b_{19}\left(r^3 - h^3\right)\Big\}\Big], \tag{4.22}$$

where $b_5, \ldots b_{23}$ are defined in the appendix.

5. Discussion of Results

It is clear that our results allow calculation of the velocity, the pressure gradient, the temperature, and the concentration field without any restrictions on the Reynolds and Weissenberg numbers but we have used a small wave number. Moreover, we note that the approximation we have used (small wave number, $\delta < 1$) holds for our application as the values of various parameters for transporting the chyme in the small intestine are [23].

$$a = 1.25\,\text{cm}, \qquad \lambda = 8.01\,\text{cm}, \qquad \delta = a/\lambda = 0.156. \tag{5.1}$$

This agrees with the small wave number approximation. In order to have an estimate of the quantitative effects of the various parameters involved in the results of the present analysis, Figures 2–23 are prepared using the MATHEMATICA package.

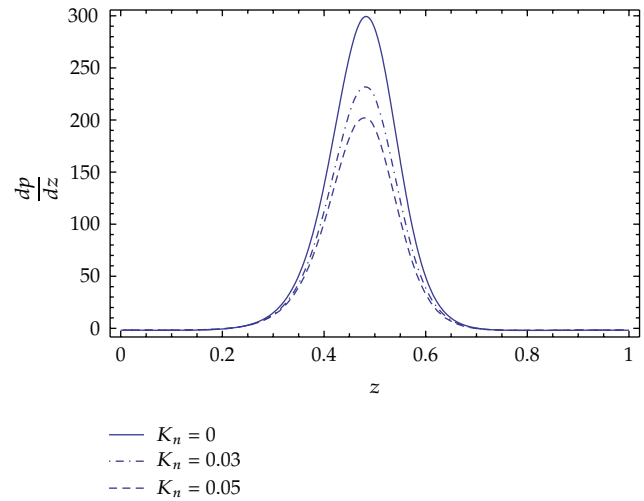

Figure 3: Pressure gradient versus z for $\varphi = 0.6$, Wi = 0.04, Re = 10, $\delta = 0.02$, $\theta = 0.1$.

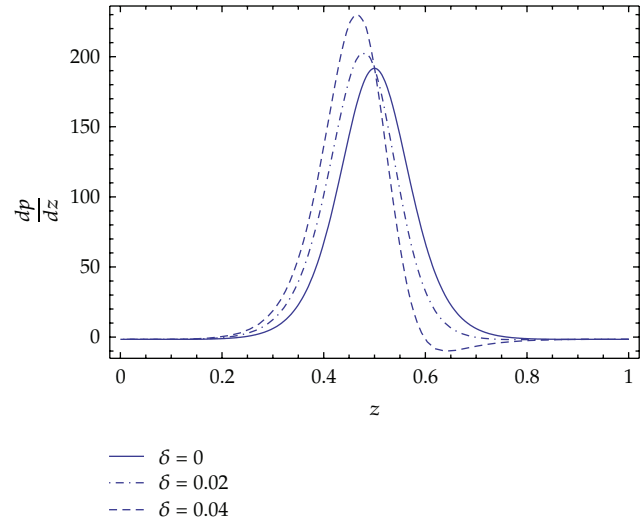

Figure 4: Pressure gradient versus z for $\varphi = 0.6$, Wi = 0.04, Re = 10, $\theta = 0.1$, $K_n = 0.05$.

5.1. Pumping Characteristics

The effect of the slip parameter K_n on the pressure gradient for both Newtonian and Oldroyd fluids is shown in Figures 2 and 3, respectively. It is evident that the pressure gradient decreases by increasing the slip parameter K_n. Furthermore, from the two figures it can be noticed that in the wider part of the tube $z \in [0, 0.3]$ and $[0.6, 1]$, the pressure gradient is small. This means that the flow can easily pass without imposition of a large pressure gradient. On the other hand, in the narrow part of the tube $z \in [0.3, 0.6]$, a large pressure gradient is required to maintain the flow to pass it.

Figures 4 and 5 illustrate the effect of wave number and Reynolds number on the pressure gradient of the Oldroyd fluid at $\theta = 0.1$, $\varphi = 0.6$, $K_n = 0.05$, Re = 10, Wi = 0.04,

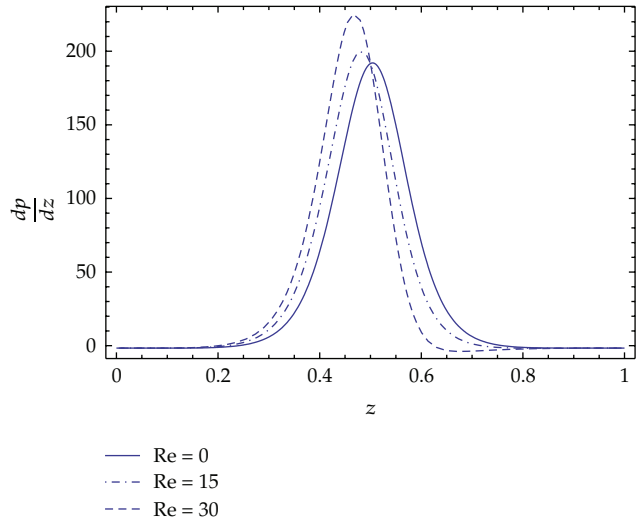

Figure 5: Pressure gradient versus z for $\varphi = 0.6$, Wi = 0.04, $\delta = 0.01$, $\theta = 0.1$, $K_n = 0.05$.

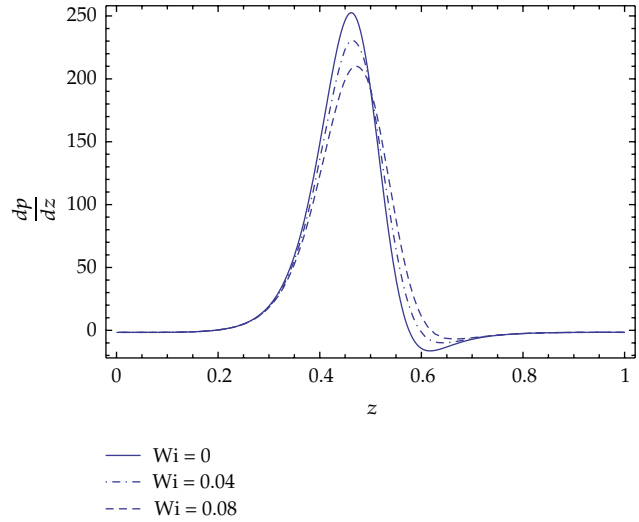

Figure 6: Pressure gradient versus z for $\varphi = 0.6$, Re = 10, $\delta = 0.02$, $\theta = 0.1$, $K_n = 0.05$.

($\delta = 0, 0.02, 0.04$) and $\theta = 0.1$, $\varphi = 0.6$, $K_n = 0.05$, Wi = 0.04, $\delta = 0.01$, (Re = $0, 15, 30$), respectively. The figures reveal that the pressure gradient increases by increasing both wave number and Reynolds number.

Figure 6 depicts the effect of the Weissenberg number Wi on the pressure gradient of the viscoelastic fluid at $\theta = 0.1$, $\varphi = 0.6$, $K_n = 0.05$, Re = 10, and $\delta = 0.02$. We can conclude that an increase in the Weissenberg number decreases the pressure gradient.

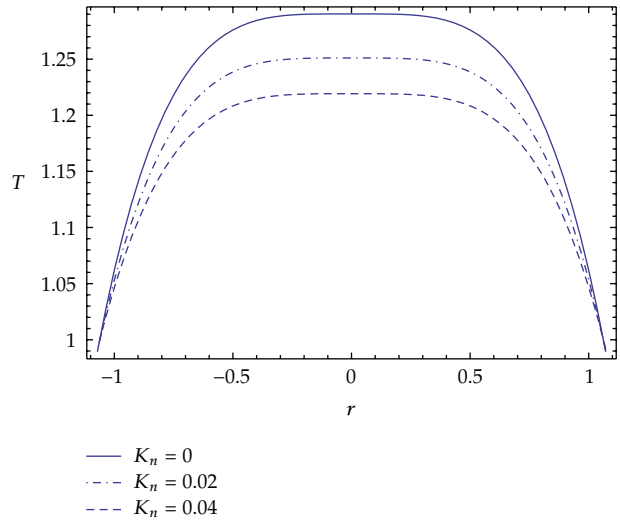

Figure 7: Temperature distribution for $z = 0.2$, Br = 1, Pr = 1, $\delta = 0$, Re = 0, Wi = 0, $\theta = 0.5$, $\phi = 0.2$.

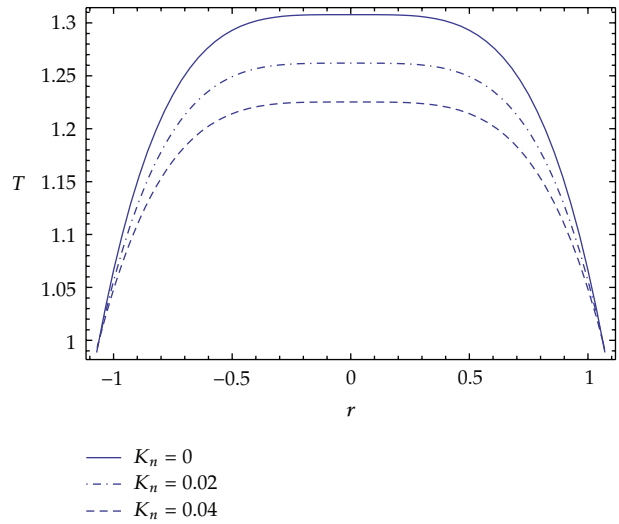

Figure 8: Temperature distribution for $z = 0.2$, Br = 1, Pr = 1, $\delta = 0.02$, Re = 10, Wi = 0.03, $\theta = 0.5$, $\varphi = 0.2$.

5.2. Temperature Distribution

Figures 7–12 are devoted to explain the effect of emerging parameters on the temperature distribution. The effect of slip parameter K_n on the temperature distribution T at $z = 0.2$, Br = 1, Pr = 1, $\theta = 0.5$, $\varphi = 0.2$ is shown in Figures 7 and 8 for both Newtonian and Oldroyd fluid, respectively. As shown, the temperature decreases as the slip parameter increases. The two figures also reveal that the behaviour of the temperature profiles is the same for both Newtonian and Oldroyd fluids.

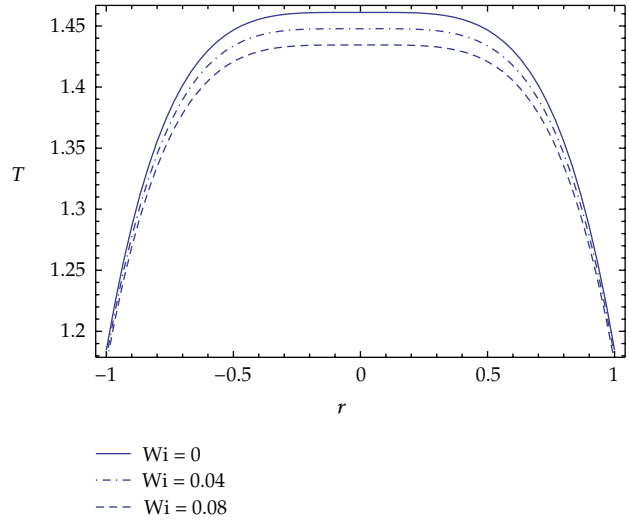

Figure 9: Temperature distribution for $z = 0.2$, Br = 1, Pr = 1, $\delta = 0.156$, Re = 10, $K_n = 0.02$, $\theta = 0.5$, $\varphi = 0.4$.

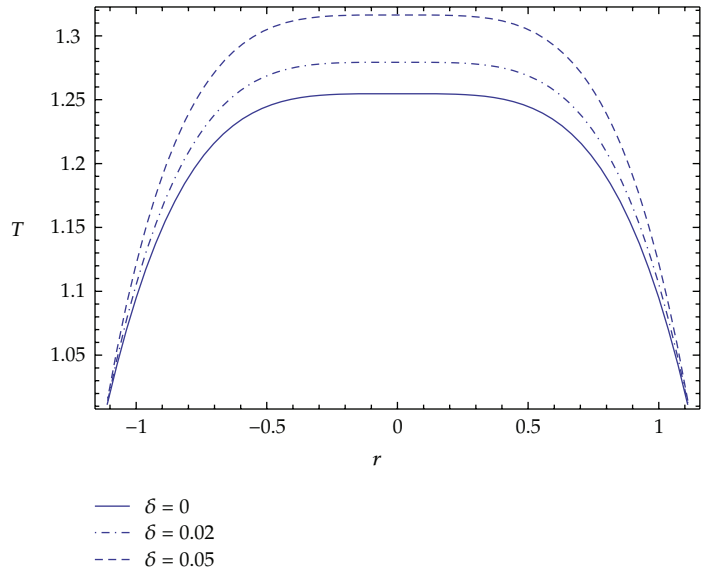

Figure 10: Temperature distribution for $z = 0.2$, Br = 1, $K_n = 0.02$, Pr = 1, Re = 10, Wi = 0.04, $\theta = 0.5$, $\varphi = 0.4$.

In Figure 9, we consider the variation of the temperature with r for $z = 0.2$, Br = 1, Pr = 1, $\theta = 0.5$, $\varphi = 0.4$, $K_n = 0.02$, $\delta = 0.156$, Re = 10, and (Wi = $0, 0.04, 0.08$). The figure shows that an increase of the Weissenberg number lowers the temperature.

The effects of the wave and Reynolds numbers on temperature distribution are shown in Figures 10 and 11, respectively. One can observe that the temperature profiles increase with increasing both wave and Reynolds numbers.

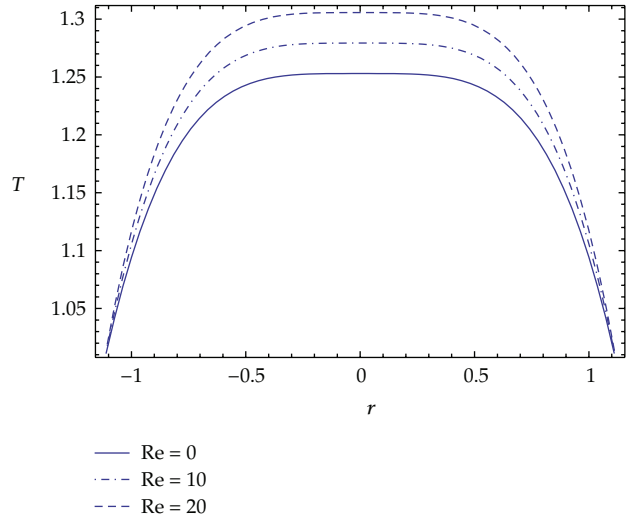

Figure 11: Temperature distribution for $z = 0.2$, Br = 1, $K_n = 0.02$, Pr = 1, $\delta = 0.02$, Wi = 0.04, $\theta = 0.5$, $\varphi = 0.4$.

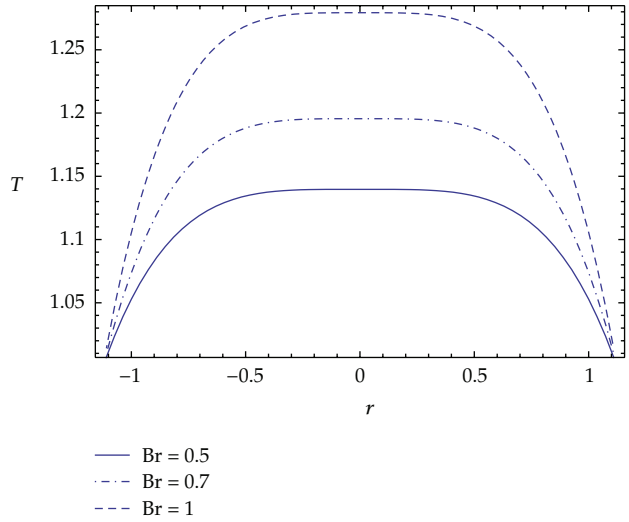

Figure 12: Temperature distribution for $z = 0.2$, Re = 10, $K_n = 0.02$, Pr = 1, $\delta = 0.02$, Wi = 0.04, $\theta = 0.5$, $\varphi = 0.4$.

In Figure 12, the temperature distribution is graphed versus r for $z = 0.2$, Re = 10, Pr = 1, $\theta = 0.5$, $\varphi = 0.4$, $K_n = 0.02$, Wi = 0.04, and (Br = 0.5, 0.7, 1). We notice that the temperature profile increases with increasing Brinkman number Br.

5.3. Concentration Profiles

Figures 13–19 illustrate the behaviour of the fluid concentration for different values of the physical parameters. Figure 3 depicts the concentration field with the variation of r for

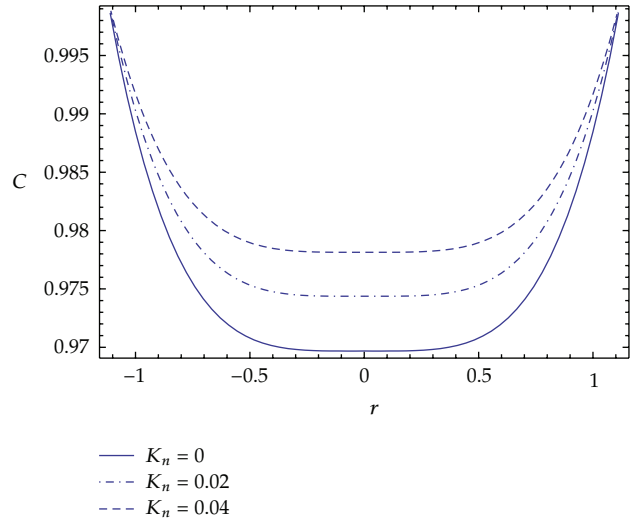

Figure 13: Concentration profiles for $z = 0.2$, Br = 1, Pr = 1, Sr = 0.3, Sc = 0.3,$\delta = 0.02$, Re = 10, Wi = 0.03, $\theta = 0.5$, $\varphi = 0.4$.

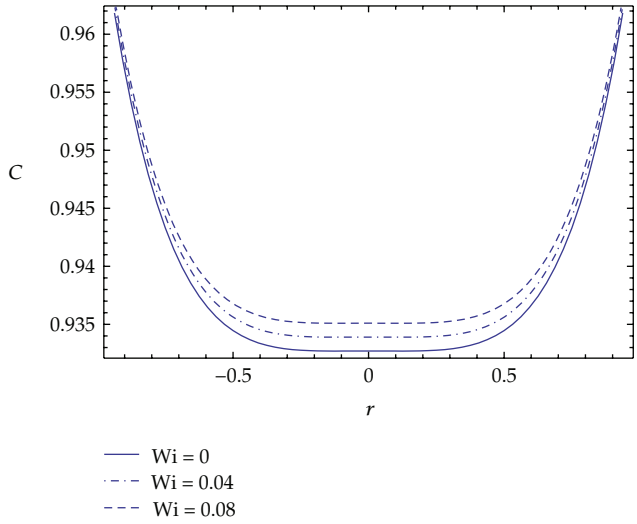

Figure 14: Concentration profiles for $z = 0.2$, Br = 1, Pr = 1, Sr = 0.3, Sc = 0.3, $\delta = 0.156$, Re = 20, $K_n = 0.02$, $\theta = 0.5$, $\varphi = 0.4$.

$z = 0.2$, Br = 1, Pr = 1, $\theta = 0.5$, $\varphi = 0.4$, Re = 10, $\delta = 0.02$, Wi = 0.03, Sr = 0.3, Sc = 0.3, and $(K_n = 0, 0.02, 0.04)$. It is observed that the concentration profiles are increasing with increasing slip parameter K_n. This means that the concentration for slip flow is greater than for no-slip flow.

Figures 14, 15, and 16 show the effects of the Weissenberg, the wave, and the Reynolds numbers on the concentration profiles. It is seen that the concentration profiles increase as the Weissenberg number increases while it decreases by increasing the wave and the Reynolds numbers.

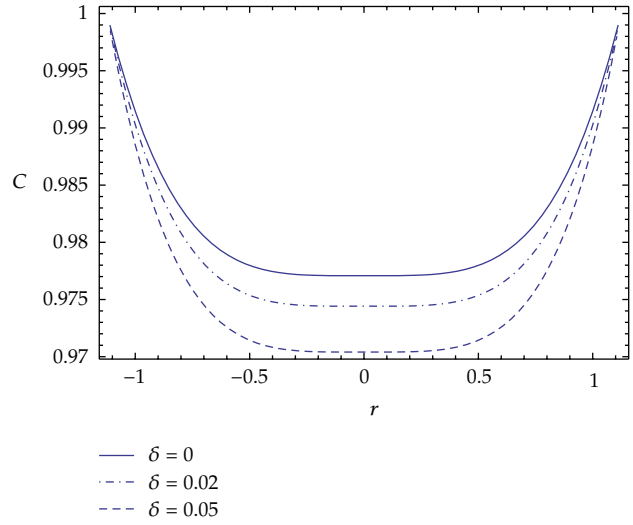

Figure 15: Concentration profiles for $z = 0.2$, Br = 1, Pr = 1, Sr = 0.3, Sc = 0.3, Re = 10, Wi = 0.04, $K_n = 0.02$, $\theta = 0.5$, $\varphi = 0.4$.

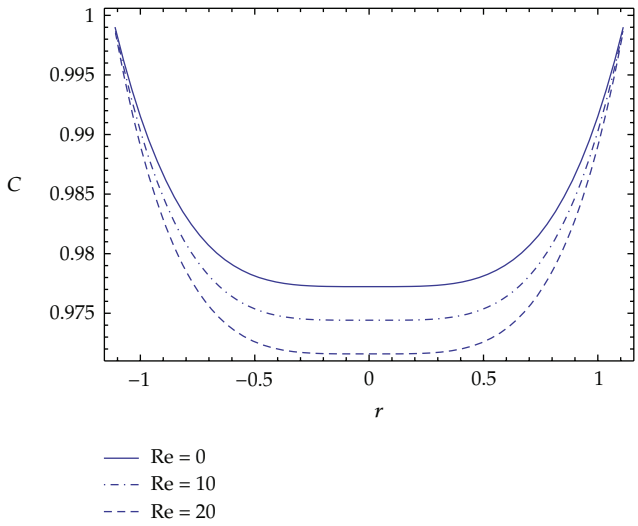

Figure 16: Concentration profiles for $z = 0.2$, Br = 1, Pr = 1, Sr = 0.3, Sc = 0.3, $\delta = 0.02$, Wi = 0.04, $K_n = 0.02$, $\theta = 0.5$, $\varphi = 0.4$.

The effects of the Brinkman, Soret, and Schmidt numbers on concentration field are shown in Figures 17, 18, and 19 for different values of other physical parameters. The figures reveal that the concentration field decreases with increasing Br, Sr, and Sc.

5.4. Streamlines and Trapping Phenomenon

The phenomenon of trapping is another interesting topic in peristaltic transport. The formulation of an internally circulating bolus of the fluid by closed streamline is called

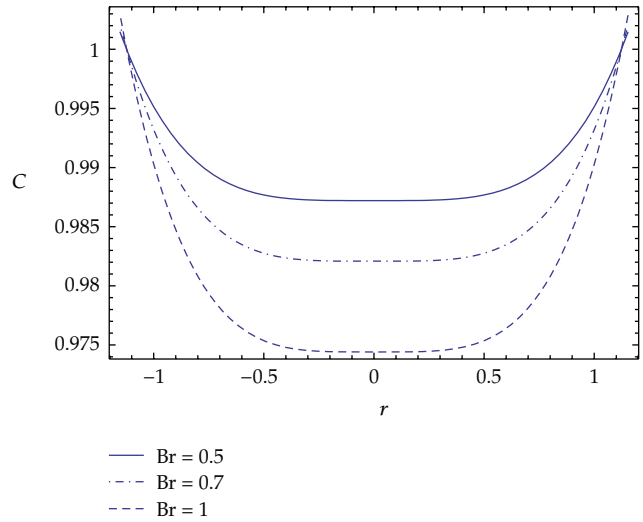

Figure 17: Concentration profiles for $z = 0.2$, Re = 10, Pr = 1, Sr = 0.3, Sc = 0.3, $\delta = 0.02$, Wi = 0.04, $K_n = 0.02$, $\theta = 0.5$, $\varphi = 0.4$.

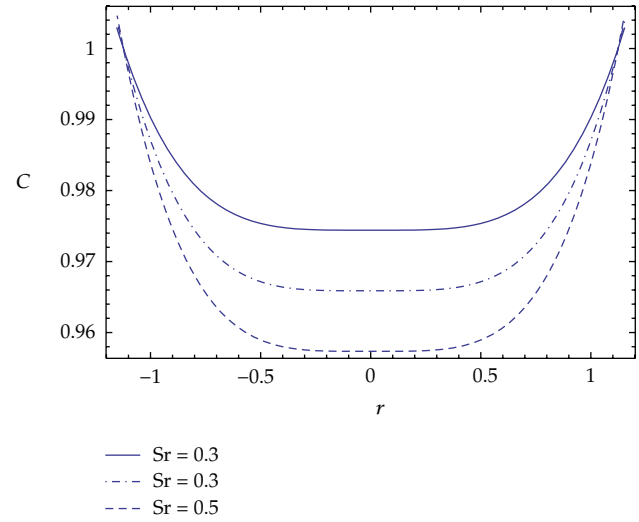

Figure 18: Concentration profiles for $z = 0.2$, Re = 10, Pr = 1, Br = 1, Sc = 0.3, $\delta = 0.02$, Wi = 0.04, $K_n = 0.02$, $\theta = 0.5$, $\varphi = 0.4$.

trapping. This trapped bolus is pulled ahead along with the peristaltic wave. The effect of slip parameter on trapping can be seen in Figure 20. It is observed that the trapping is symmetric about the centre line and the volume of the trapped bolus decreases with increasing K_n.

Figures 21 and 22 illustrate the effects of the wave and Reynolds numbers on the streamline at fixed values of other parameters. It is evident that the volume of the trapped bolus increases by increasing δ and Re. Moreover, we notice from the two figures that when δ andRe increase, another trapped bolus arises.

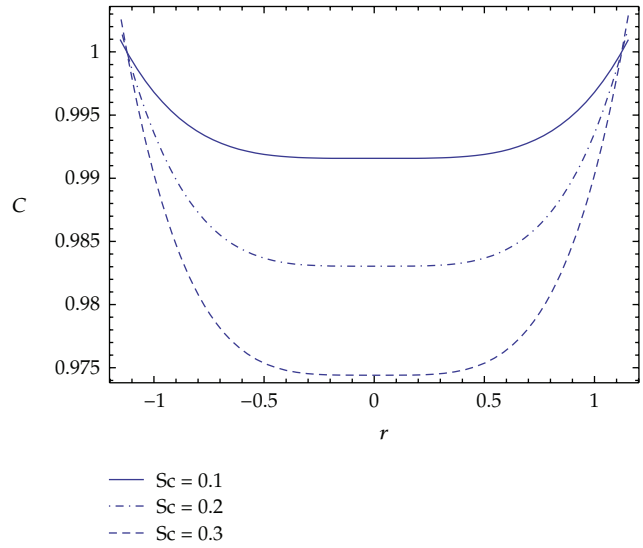

Figure 19: Concentration profiles for $z = 0.2$, Re $= 10$, Pr $= 1$, Br $= 1$, Sr $= 0.3$, $\delta = 0.02$, Wi $= 0.04$, $K_n = 0.02$, $\theta = 0.5$, $\varphi = 0.4$.

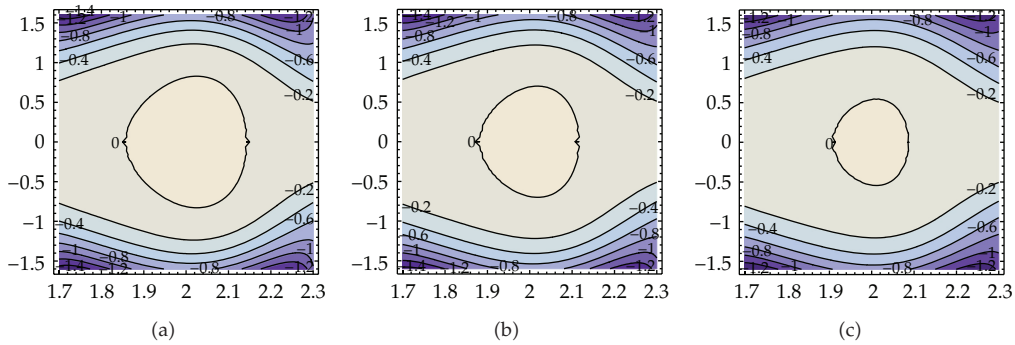

Figure 20: Streamlines for Wi $= 0.03$, Re $= 10$, $\delta = 0.02$, $\theta = 0.3$, $\varphi = 0.4$, $K_n = (0, 0.05, 0.1)$.

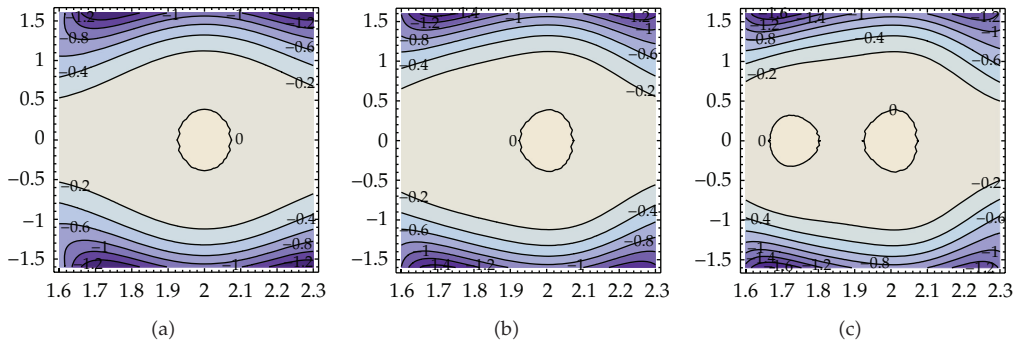

Figure 21: Streamlines for Wi $= 0.03$, Re $= 10$, $K_n = 0.05$, $\theta = 0.3$, $\varphi = 0.3$, $\delta = (0, 0.03, 0.05)$.

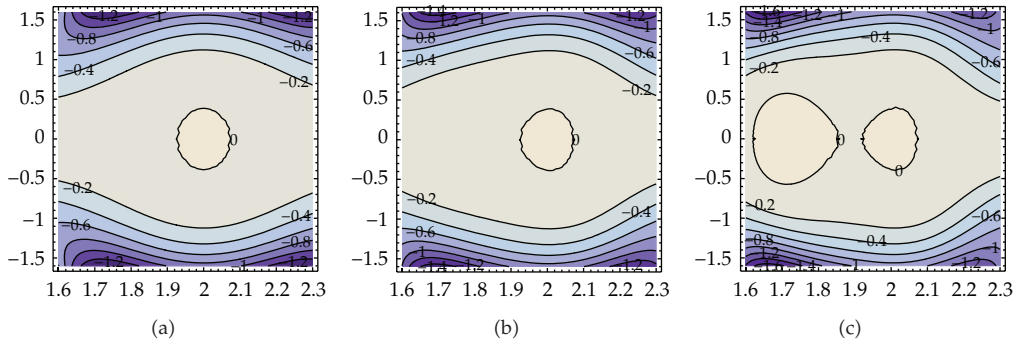

Figure 22: Streamlines for Wi = 0.03, $K_n = 0.05$, $\delta = 0.03$, $\theta = 0.3$, $\varphi = 0.3$, Re = (0, 10, 20).

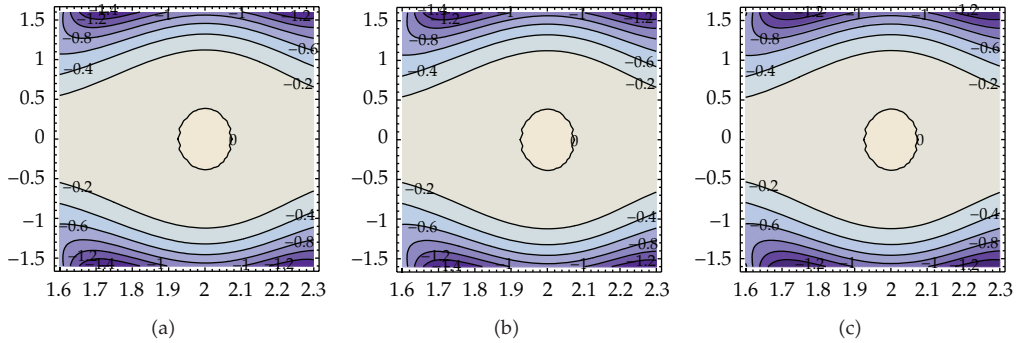

Figure 23: Streamlines for Re = 1, $\delta = 0.05$, $\varphi = 0.3$, $\theta = 0.3$, $K_n = 0.05$, Wi = (0, 0.04, 0.08).

Finally, Figure 23 shows the graph of streamlines for $\theta = 0.3$, $\varphi = 0.3$, $\delta = 0.05$, Re = 1, $K_n = 0.05$, and (Wi = 0, 0.04, 0.08). As shown, there is no effect of the Weissenberg number on the behaviour of streamlines.

6. Conclusion

The study examines the combined effect of slip velocity and heat and mass transfer on peristaltic transport of a viscoelastic fluid (Oldroyd fluid) in uniform tube. The problem can be considered as an application to the movement of chyme in small intestine. Using perturbation technique, analytical solutions for velocity, pressure gradient, temperature, and concentration fields have been derived without any restrictions on Reynolds number and Weissenberg number. The main results are summarized as follows.

(1) The pressure gradient decreases by increasing the slip parameter K_n.

(2) The pressure gradient increases with increasing the wave and Reynolds numbers while it decreases with increasing the Weissenberg number.

(3) The temperature profiles decrease as the slip parameter K_n increases.

(4) The temperature profiles decrease by increasing the Weissenberg number.

(5) The temperature profiles increase with increasing the wave, the Reynolds, and the Brinkman numbers.

(6) The concentration profiles are increasing when the slip parameter and Weissenberg number increase while it is decreasing when the wave, the Reynolds, the Brinkman, the Eckert, and the Soret numbers are increasing.

(7) The trapped bolus decreases with increasing slip parameter and increases with increasing wave number and Reynolds number.

Appendix

$$a_1 = -\frac{2(2f_0 + h^2)}{(h^4 + 4h^3K_n)}, \qquad a_2 = -a_1\left(h^2 + 2hK_n\right) - 1, \qquad a_3 = -\frac{a_1'}{4}, \qquad a_4 = -\frac{a_2'}{2},$$

$$a_5 = \frac{(2a_1a_3 + a_1a_1')}{36}, \qquad a_6 = \frac{(2a_1a_4 + a_1a_2' + a_2a_1')}{16}, \qquad a_7 = \frac{a_2a_2'}{4},$$

$$a_8 = -\left(h^6 + 6K_nh^5\right)a_5 - \left(h^4 + 4K_nh^3\right)a_6 - \left(h^2 + 2K_nh\right)a_7, \qquad a_9 = -\frac{(4a_1a_3 + a_1a_1')}{2},$$

$$a_{10} = a_2a_1', \qquad a_{11} = -\left(h^4 + 4K_nh^3\right)a_9 - \left(h^2 + 2K_nh\right)a_{10}, \qquad a_{12} = \left(\frac{9a_1a_5}{32}\mathrm{Pr} + \frac{3a_1a_5}{8}\right),$$

$$a_{13} = \left(\frac{2a_1^2a_4 + a_1a_2a_1'}{72}\mathrm{Pr} + \frac{4a_1a_6}{9}\right), \qquad a_{14} = \left(\frac{a_1a_7}{2} - \frac{a_1^2a_1'h^4}{32}\mathrm{Pr}\right), \qquad a_{15} = -\frac{a_1a_{10}}{8}\mathrm{Pr},$$

$$a_{16} = \frac{(4a_1a_9 + 2a_1^2a_1')}{9}, \qquad a_{17} = \frac{(8a_1a_3 - 2a_1a_1')}{25}, \qquad a_{18} = \frac{(a_1a_{10} + a_1^2a_2')}{2},$$

$$a_{19} = -\frac{2a_{10}}{9}, \qquad a_{20} = a_{12} + \frac{9a_1a_5}{32}\mathrm{Sc}, \qquad a_{21} = a_{13} + \frac{(2a_1^2a_4 + a_1a_1'a_2)}{72}\mathrm{Sc},$$

$$a_{22} = a_{14} - \frac{a_1^2a_1'h^4}{32}\mathrm{Sc}, \qquad a_{23} = a_{15} - \frac{a_1a_{10}h^4}{8}\mathrm{Sc},$$

$$b_1 = -\frac{2(2f + h^2)}{(h^4 + 4h^3K_n)}, \qquad b_2 = -b_1\left(h^2 + 2hK_n\right) - 1, \qquad b_3 = -\frac{b_1'}{4},$$

$$b_4 = -\frac{b_2'}{2}, \qquad b_5 = \frac{(2b_1b_3 + b_1b_1')}{36}, \qquad b_6 = \frac{(2b_1b_4 + b_1b_2' + b_2b_1')}{16}, \qquad b_7 = \frac{b_2b_2'}{4},$$

$$b_8 = -\left(h^6 + 6K_nh^5\right)b_5 - \left(h^4 + 4K_nh^3\right)b_6 - \left(h^2 + 2K_nh\right)b_7, \qquad b_9 = -\frac{(4b_1b_3 + b_1b_1')}{2},$$

$$b_{10} = b_2b_1', \qquad b_{11} = -\left(h^4 + 4K_nh^3\right)b_9 - \left(h^2 + 2K_nh\right)b_{10}, \qquad b_{12} = \left(\frac{9b_1b_5}{32}\mathrm{Pr} + \frac{3b_1b_5}{8}\right),$$

$$b_{13} = \left(\frac{2b_1^2b_4 + b_1b_2b_1'}{72}\mathrm{Pr} + \frac{4b_1b_6}{9}\right), \qquad b_{14} = \left(\frac{b_1b_7}{2} - \frac{b_1^2b_1'h^4}{32}\mathrm{Pr}\right), \qquad b_{15} = -\frac{b_1b_{10}}{8}\mathrm{Pr},$$

$$b_{16} = \frac{(4b_1b_9 + 2b_1^2b_1')}{9}, \qquad b_{17} = \frac{(8b_1b_3 - 2b_1b_1')}{25}, \qquad b_{18} = \frac{(b_1b_{10} + b_1^2b_2')}{2},$$

$$b_{19} = -\frac{2b_{10}}{9}, \qquad b_{20} = b_{12} + \frac{9b_1b_5}{32}\mathrm{Sc}, \qquad b_{21} = b_{13} + \frac{\left(2b_1^2b_4 + b_1b_1'b_2\right)}{72}\mathrm{Sc},$$

$$b_{22} = b_{14} - \frac{b_1^2b_1'h^4}{32}\mathrm{Sc}, \qquad b_{23} = b_{15} - \frac{b_1b_{10}h^4}{8}\mathrm{Sc}. \tag{A.1}$$

Acknowledgments

The author would like to thank Professor Dr. Engineer Rolf Radespiel, Head of the Institute of Fluid Mechanics, TU Braunschweig, for his invaluable discussions and constant support. Furthermore, the author thanks the DAAD for financial support to his research visit to Germany where this work was accomplished.

References

[1] E. F. Elshehawey, A. M. F. Sobh, and E. M. E. Elbarbary, "Peristaltic motion of a generalized Newtonian fluid through a porous medium," *Journal of the Physical Society of Japan*, vol. 69, no. 2, pp. 401–407, 2000.

[2] D. Tsiklauri and I. Beresnev, "Non-newtonian effects in the peristaltic flow of a Maxwell fluid," *Physical Review E*, vol. 64, no. 3, part 2, Article ID 036303, 2001.

[3] T. Hayat, Y. Wang, A. M. Siddiqui, K. Hutter, and S. Asghar, "Peristaltic transport of a third-order fluid in a circular cylindrical tube," *Mathematical Models and Methods in Applied Sciences*, vol. 12, no. 12, pp. 1691–1706, 2002.

[4] A. H. Abd El Naby, A. E. M. El Misery, and M. F. Abd El Kareem, "Separation in the flow through peristaltic motion of a Carreau fluid in uniform tube," *Physica A*, vol. 343, no. 1–4, pp. 1–14, 2004.

[5] K. Vajravelu, S. Sreenadh, and V. R. Babu, "Peristaltic transport of a Herschel-Bulkley fluid in an inclined tube," *International Journal of Non-Linear Mechanics*, vol. 40, no. 1, pp. 83–90, 2005.

[6] T. Hayat and N. Ali, "On mechanism of peristaltic flows for power-law fluids," *Physica A*, vol. 371, no. 2, pp. 188–194, 2006.

[7] T. Hayat, M. Khan, A. M. Siddiqui, and S. Asghar, "Non-linear peristaltic flow of a non-Newtonian fluid under effect of a magnetic field in a planar channel," *Communications in Nonlinear Science & Numerical Simulation*, vol. 12, no. 6, pp. 910–919, 2007.

[8] A. M. Sobh, "Interaction of couple stresses and slip flow on peristaltic transport in uniform and nonuniform channels," *Turkish Journal of Engineering & Environmental Sciences*, vol. 32, no. 2, pp. 117–123, 2008.

[9] Md. A. Ikbal, S. Chakravarty, and P. K. Mandal, "An unsteady peristaltic transport phenomenon of non-Newtonian fluid—a generalised approach," *Applied Mathematics & Computation*, vol. 201, no. 1-2, pp. 16–34, 2008.

[10] M. Kothandapani and S. Srinivas, "Non-linear peristaltic transport of a Newtonian fluid in an inclined asymmetric channel through a porous medium," *Physics Letters A*, vol. 372, no. 8, pp. 1265–1276, 2008.

[11] S. Srinivas and M. Kothandapani, "The influence of heat and mass transfer on MHD peristaltic flow through a porous space with compliant walls," *Applied Mathematics & Computation*, vol. 213, no. 1, pp. 197–208, 2009.

[12] N. T. M. Eldabe, M. F. El-Sayed, A. Y. Ghaly, and H. M. Sayed, "Mixed convective heat and mass transfer in a non-Newtonian fluid at a peristaltic surface with temperature-dependent viscosity," *Archive of Applied Mechanics*, vol. 78, no. 8, pp. 599–624, 2008.

[13] S. Nadeem and N. S. Akbar, "Influence of radially varying MHD on the peristaltic flow in an annulus with heat and mass transfer," *Journal of the Taiwan Institute of Chemical Engineers*, vol. 41, no. 3, pp. 286–294, 2010.

[14] N. S. Akbar, S. Nadeem, T. Hayat, and A. A. Hendi, "Effects of heat and mass transfer on the peristaltic flow of hyperbolic tangent fluid in an annulus," *International Journal of Heat and Mass Transfer*, vol. 54, no. 19-20, pp. 4360–4369, 2011.

[15] T. Hayat, S. Noreen, M. Alhothuali, S. Asghar, and A. Alhomaidan, "Peristaltic flow under the effects of an induced magnetic field and heat and mass transfer," *International Journal of Heat & Mass Transfer*, vol. 55, pp. 443–452, 2012.

[16] T. Hayat, S. Hina, A. A. Hendi, and S. Asghar, "Effect of wall properties on the peristaltic flow of a third grade fluid in a curved channel with heat and mass transfer," *International Journal of Heat & Mass Transfer*, vol. 54, pp. 3511–3521, 2012.
[17] A. M. Sobh, "Slip flow in peristaltic transport of a Carreau fluid in an asymmetric channel," *Canadian Journal of Physics*, vol. 87, no. 8, pp. 957–965, 2009.
[18] T. Hayat and O. U. Mehmood, "Slip effects on MHD flow of third order fluid in a planar channel," *Communications in Nonlinear Science and Numerical Simulation*, vol. 16, no. 3, pp. 1363–1377, 2011.
[19] S. Noreen, T. Hayat, and A. Alsaedi, "Study of slip and induced magnetic field on the peristaltic flow of pseudoplastic fluid," *International Journal of Physical Sciences*, vol. 6, pp. 8018–8026, 2011.
[20] T. Hayat, N. Saleem, and A. A. Hendi, "A mathematical model for studying the slip effect on peristaltic motion with heat and mass transfer," *Chinese Physics Letters*, vol. 28, no. 3, Article ID 034702, 4 pages, 2011.
[21] N. Saleem, T. Hayat, and A. Alsaedi, "Effects of induced magnetic field and slip condition on peristaltic transport with heat and mass transfer in a non-uniform channel," *International Journal of Physical Sciences*, vol. 7, pp. 191–204, 2012.
[22] R. K. Rathy, *An Introduction to Fluid Dynamics*, IBH Publishing, New Delhi, India, 1976.
[23] L. M. Srivastava and V. P. Srivastava, "Peristaltic transport of a non-Newtonian fluid: applications to the vas deferens and small intestine," *Annals of Biomedical Engineering*, vol. 13, no. 2, pp. 137–153, 1985.